Letters in Applied NanoBioScience
Open-Access Journal (ISSN: 2284-6808)

Article
Volume 13, Issue 4, 2024, 153
https://doi.org/10.33263/LIANBS134.153

Identification of Potent New Brain Cancer EGFR Inhibitor from Usimine A and Usimine B: Computer-Aided Drug Design Perspective

Miah Roney [1,2], Abdul Rashid Issahaku [3], Anke Wilhelm [3], Mohd Fadhlizil Fasihi Mohd Aluwi [1,2,*]

[1] Faculty of Industrial Sciences and Technology, Universiti Malaysia Pahang Al-Sultan Abdullah, Lebuhraya Tun Razak, 26300 Gambang, Kuantan, Pahang Darul Makmur, Malaysia
[2] Bio Aromatic Research Centre, Universiti Malaysia Pahang Al-Sultan Abdullah, Lebuhraya Tun Razak, 26300 Gambang, Kuantan, Pahang Darul Makmur, Malaysia
[3] Department of Chemistry, University of the Free State, 205 Nelson Mandela Avenue, Bloemfontein 9301, South Africa
* Correspondence: fasihi@umpsa.edu.my

Scopus Author ID 56254778800
Received: 26.11.2023; Accepted: 12.05.2024; Published: 24.08.2024

Brain cancer ranks 10th among cancer-related causes of death for patients worldwide. Medical chemists still have many challenges because of the high side effects, increasing tumor resistance, and low selectivity of new chemotherapeutic medications despite the enormous effort put out to extract, develop, and synthesize them. The anti-cancer potential of many natural substances has garnered significant research in the past few decades. This study's main goal is to discover the anti-cancer activity of Usimine A and Usimine B against the EGFR protein of brain cancer using the in-silico approaches. In this study, the biological features of Usimine A and Usimine B were determined using the PASS prediction tool, and the pIC50 value was predicted to know the activity of these compounds. Furthermore, molecular docking and dynamic simulations were performed to see the binding affinity and stability of the docking complexes. Usimine A and Usimine B have the PASS prediction score of 0.835<Pa<0.002 and 0.851<Pa<0.002, respectively. Additionally, the QSAR analysis demonstrated that both compounds have respective pIC50 values of 4.82 and 4.74. Furthermore, the docking calculations demonstrated the remarkable efficacy of Usimine B (-7.3 kcal/mol) as an EGFR inhibitor of brain tumors. This compound exhibited five hydrogen bonds with the residues of Leu792, Met793, Asn842, Thr854, and Val843 in the active site of EGFR protein. A 200 ns molecular dynamic simulation demonstrated the stability of the Usimine B-EGFR complex compared to the reference complex (Gefitinib-EGFR). Furthermore, the thermodynamic calculations of the Usimine B-EGFR complex exhibited a binding affinity of -28.69± 3.50 kcal/mol for the EGFR protein. The results show that Usimine B has been identified as an inhibitor of brain cancer against EGFR protein. As part of the process of identifying and developing a novel medicine against brain cancer, more studies on in vitro and in vivo Usimine B is advised.

Keywords: in-silico; Usimine A; Usimine B; EGFR; docking; MD simulation.

1. Introduction

Global statistics show that, after infectious, parasitic, and cardiovascular diseases, cancer is the third most deadly sickness globally. The fact that 19.3 million people had cancer treatment in 2020 indicates that there is still a significant danger of the disease for people worldwide [1]. Among them is brain cancer, a tumor located in the brain or central spinal canal that is classified as an intracranial solid neoplasm. Brain tumors can be classified as either

primary or metastatic (secondary), depending on where in the body the cancer cells that cause them have spread. Primary brain tumors start in the brain. Primary brain cancer never spreads outside of the central nervous system; instead, it dies from unchecked tumor development inside the skull's constrained area [2]. Between 4 and 10/100,000 people in the general population are affected by primary cerebral malignancies, which account for 2.3% of all cancer-related deaths and 1.4% of all cancers. In this regard, brain metastasis significantly increases the mortality of brain tumors [3]. Cancer-related medical needs continue to be one of the most challenging fields of research.

Together with surgery, radiation therapy, and antibody-based immunotherapy, chemotherapy is a cornerstone of cancer treatment. Many cancer patients experience failure with conventional chemotherapy for a variety of reasons, with drug resistance and severe side effects being the primary culprits [4]. As a result, drug research works tirelessly to enhance treatment outcomes through the preclinical creation of novel medications and the clinical optimization of treatment plans. The epidermal growth factor receptor (EGFR) gene is amplified in glioblastoma multiforme-GBM at a frequency of about 50-60% [5]. This amplification is frequently linked to a mutation specific to the tumor that encodes a shortened form of the receptor called ΔEGFR (also called de2-7EGFR or EGFRvIII), which results in constitutive tyrosine kinase activity without the need for a ligand. GBM patients have a worse overall survival rate when their expression of ΔEGFR is expressed, and it is associated with glioma cell migration, tumor development, invasion, survival, and resistance to therapy [6]. Drug resistance caused by EGFR is not limited to well-known anti-cancer medications; it can also be directed towards alternative cytotoxic substances found in nature. Accordingly, EGFR-mediated resistance might be a form of generic cellular defense mechanism against a wide variety of harmful xenobiotics [4].

Natural products have long been significant in the field of cancer pharmacology. In addition to being well-known cytotoxic anti-cancer medications (such as taxanes, vinca alkaloids, anthracyclines, and camptothecins), they are also valuable lead compounds for the creation of cutting-edge, targeted chemotherapy techniques [4]. These environmental conditions lead to the range of secondary metabolites produced by lichens [7]. Lichens have been used for food, dyes, decorations, and several traditional medicines since prehistoric times. Moreover, as various studies have shown, lichens are composed of a range of secondary metabolites that possess antibacterial, antiviral, analgesic, antipyretic, antiproliferative, cytotoxic, and antioxidant properties [8]. The main metabolic processes for lichen chemicals are poly-malonyl, shikimate, and mevalonic acid. Numerous interesting and unique phenolic structures, such as dibenzofurans, depsides, depsidones, depsones, quinones, and derivatives of pulvinic acid, have been created by these routes [9]. The current study outlines the anti-breast cancer activity of Usimine A and Usimine B (Figure 1), which were isolated and recently characterized from the Antarctic lichen Ramalina terebrata [10].

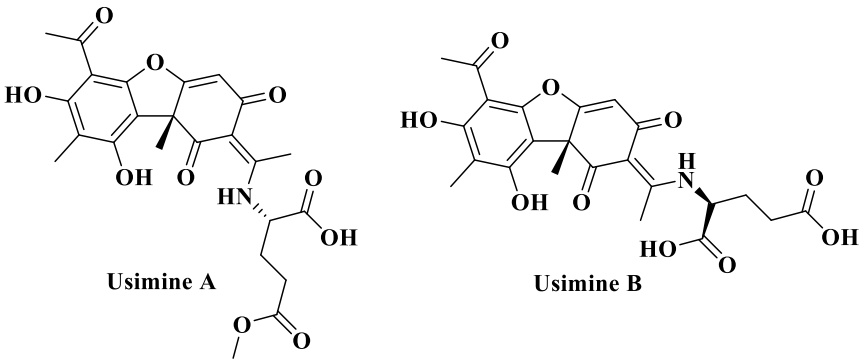

Figure 1. The structure of Usimine A and Usimine B.

In-silico techniques, including PASS prediction, QSAR, molecular docking, and a molecular dynamic based on receptors, were used to determine the molecular activity of these drugs on specific brain cancer receptors. The study results demonstrate that Usimine A and Usimine B can interact with EGFR, the brain cancer receptor, to offer a potential treatment. Furthermore, the Usimine B-EGFR complex was stable.

2. Materials and Methods

2.1. Prediction of anti-cancer properties.

The selected compounds underwent examination using the PASS online web server (http://www.way2drug.com) to determine their possible biological features. Based on the structural–activity link between the chemical of interest and a training set of more than 26,000 compounds with known biological activities, PASS ascertains the pertinent biological activities of compounds [11]. Pa (probable activity) and Pi (probable inactivity) values, which range from 0.000 to 1.000 for Pa and Pi, respectively, were used to characterize the compounds' possible biological features. It is worthwhile to investigate the pharmacological activity when Pa > 0.7 and larger than Pi for a certain drug activity [12].

2.2. Calculation of QSAR and pIC_{50}.

The QSAR creates a connection between the chemical structure and biological activity of chemical compounds [13-15]. Furthermore, the QSAR is a quantum chemistry technique that forecasts a compound's potential for use in drug discovery and development. We utilized the publicly accessible ChemDes website (http://www.scbdd.com/chemopy_desc/index/) to perform QSAR and pIC_{50} [16]. Chiv5 mean molecular connectivity, bcutm1 mean burden descriptors, MRVSA9, MRVSA6, and PEOEVSA5 are MOE type descriptors; GATSv4 indicates autocorrelation descriptors; the final two parameters, J and diameter, suggest topological descriptors of drug molecules for reported ligands. These web services provided data in these forms. The aforementioned parameters were first gathered from the ChemDes database in order to determine and calculate the QSAR and pIC_{50}. Next, the multiple linear regression (MLR) was developed in an Excel sheet, and the pIC_{50} value was calculated using the MLR equations.

pIC_{50} (Activity)= -2.768483965 + 0.133928895 × (Chiv5) + 1.59986423 × (bcutm1) + (-0.02309681) × (MRVSA9) + (-0.002946101) × (MRVSA6) + (0.00671218) × (PEOEVSA5) + (-0.15963415) × (GATSv4) + (0.207949857) × (J) + (0.082568569) × (Diametert) [16]. (1)

2.3. Molecular docking.

Using the online docking tool CB-Dock, the previously described methodologies were employed to estimate the docking analysis [17]. The study conducted by Yan et al. investigated the interactions between Usimine A and Usimine B and the EGFR 696-1022 T790M (PDB ID: 5XDK) [18]. The .mol file of compounds and the .pdb file of the target protein were entered into this program. The compounds and the reference drug's structures were built using ChemSketch software and stored in .mol format. Additionally, the PDB format was used to retrieve and preserve the target proteins' 3D structure. The CB-Dock technique accurately locates the binding zone, ascertains the size and position of the center, modifies the size of the docking region based on the molecules supplied, and then uses AutoDock Vina version 1.1.2 to dock [19]. A PBD file for the receptor and a. mol file for the ligands were entered prior to docking. Each of the several top cavities that were automatically selected throughout this process and used for additional research (cavity sorting) underwent molecular docking.

2.4. Molecular dynamic (MD) simulation.

Using the Assisted Model Building with Energy Refinement (AMBER18) suit, a 200 ns molecular dynamics (MD) simulation was conducted using the complexes of Usimine B-EGFR, which had the highest docking score, and Gefitinib-EGFR, which was the reference molecule [20]. Additionally, an unbound Apo was made ready for simulation. The FF14SB force field in AMBER was utilized to parameterize the systems. The integrated pdb4amber program was also used to modify, rename, and protonate the protein. By using the ANTECHAMBER module to generate atomic partial charges for the compounds, the compounds were similarly parametrized. The Link Edit and Parametrize module of the AMBER18 package was then used to create the topology and parameter files for the complexes. Using a water box measuring 8 Å, the Transferable Intermolecular Potential with 3 Points (TIP3P) module was also utilized to solve the complexes and neutralize them by injecting Na^+ and Cl^- counter ions. Next, using a 500 kcal/mol energy restraint potential, the systems were partially reduced for 2500 steps before being minimized for 5000 steps without any energy constraints. The systems were then gradually heated using a Langevin thermostat [21] with a harmonic constraint of 5 kcal/mol Å from 0 K to 300 K for 50 ps in the conventional moles (N), volume (V), and temperature (T) ensemble. The systems were equilibrated at 300 K for 1000 ps without energy limitation at a fixed atmospheric pressure of 1 bar. The trajectory data was analyzed using Amber18's CPPTRAJ module.

2.5. Thermodynamics calculation.

Because of its well-established efficacy and dependability, the Molecular Mechanics/Poisson-Boltzmann Surface Area (MM/PBSA) approach was utilized to examine the compounds' binding to the proteins [21]. In relation to the binding, stability, and affinity of the compounds, this gives estimations of the free binding energies involved in the complex formation. The free binding energy can be represented mathematically as follows:

$$\Delta G_{bind} = G_{complex} - G_{receptor} - G_{ligand} \quad (2)$$

$$\Delta G_{bind} = E_{gas} + G_{sol} - T\Delta S \quad (3)$$

$$Egas = E_{int} + E_{vdw} + E_{ele} \quad (4)$$

$$Gsol = G_{PB} + G_{non\text{-}polar} \quad (5)$$

$$G_{non\text{-}polar} = \gamma SASA + b \quad (6)$$

Where ΔG_{bind}: sum of the gas phase and solvation; $T\Delta S$: entropy; E_{gas}: total of the AMBER force field internal energy; E_{int}: bond, angle, and torsion; E_{vdw}: ovalent van-der Waals; E_{ele}: non-bonded electrostatic energy; G_{PB}: polar solvation contribution; $G_{non-polar}$: nonpolar contribution energy.

Moreover, per-residue breakdown investigations were carried out to calculate the specific energy contribution that each substrate pocket residue made to the compounds' affinity and stabilization.

3. Results and Discussion

3.1. Prediction of anti-cancer properties.

Based on their structures, the Pass online biological activity prediction program was used to assess the PASS prediction of Usimine A and Usimine B. According to Table **1**, these substances may have pharmacological effects (Pa > Pi), including the ability to prevent brain tumors. If Pa is greater than Pi, the activity of a lead molecule is deemed experimental. Pa values between 0.5 and 0.6 show notable pharmacological potentials, whereas Pa > 0.6 indicates a significant likelihood of pharmacological potential [12]. A Pa value of 0.5 indicates a decrease in pharmacological activity, which may result in identifying a new compound. Pa > Pi was seen in the compounds found using SAF-CFE, indicating their pharmacological action. According to predictions, the compounds Usimine A and Usimine B have anti-cancer properties, with probability activities (Pa) > 0.7 and Pa > Pi (probable inactivity). With a Pa of >0.7 and Pi of <0.005, it was projected that the compounds Usimine A and Usimine B would act as anti-cancer agents against brain cancer. Further experimental testing is necessary since these compounds have the potential to be effective anti-cancer agents against brain cancer, as shown by their Pa > Pi.

Table 1. PASS prediction of biological activities of selected compounds.

Compound Name	Biological Activity	Pa	Pi
Usimine A	Brain Cancer	0.835	0.002
Usimine B	Brain Cancer	0.851	0.002

3.2. Calculation of QSAR and pIC_{50}.

In order to forecast the biological activity of chemical compounds based on their molecular structures, computer modeling techniques such as QSAR have been utilized in drug discovery and design [14]. This is completed and mostly applied to creating novel medications, particularly computer-aided drug design. It entails creating mathematical models that relate structural features or physicochemical descriptions of molecules to how they function biologically [22,23].

The QSAR standard ranges are regarded as being less than 10. Theoretically, every molecule with a value less than 10 is potential [16].

Table 2. Data of QSAR calculation.

Compound Name	Chiv5	bcutm1	(MRVSA9)	(MRVSA6)	(PEOEVSA5)	GATSv4	J	Diameter	pIC_{50}
Usimine A	2.981	4.061	29.288	39.796	0.0	0.806	1.853	15.0	4.82
Usimine B	2.928	4.061	29.288	39.796	0.0	0.804	1.875	14.0	4.74

3.3. Molecular docking.

The QSAR and pIC50 overall results in our present analysis are positive (Table 2) and satisfied with standard ranges. Usimine A and Usimine B had pIC50 values of 4.82 and 4.74, respectively. These compounds may be therapeutically effective against the targeted illness, according to the pIC50 results.

The results of molecular docking are often presented in terms of the degree to which medicines bind to receptors and the number of hydrophobic, polar, and nonpolar bonds that form between them during docking [24]. Using the online docking program CB-Dock, molecular docking studies were conducted for the investigated drugs against the EGFR protein (PDB ID: 5XDK). The docking data were then assessed using the vina score function, and comparisons between the tested compounds and the reference medication (Gefitinib) were made using the hydrogen bonds and hydrophobic interactions between the tested compounds and the target receptor.

Usimine A and Usimine B were found to have minimum binding energy ranging from -6.8 to -7.3 kcal/mol against the EGFR 696-1022 T790M protein of brain cancer (Table 3). Therefore, these molecules could have a comparable inhibitory potential to the enzyme studied with the reference compound Gefitinib (-7.7 kcal/mol). UA was found to have hydrogen bonding interaction with Asp1014, Gln791, Pro772, Asn771 and Lys852 amino acid residues and hydrophobic interaction with Leu778, Gln791, Leu1017, Asp1014, Pro722, Arg766 and Asn771amino acid residues (Figure 2 (B)). Usimine A docked into the active site of the target protein with the binding energy of -6.9 kcal/mol and mediated one hydrogen bond with Ala1013 residue and four hydrophobic interactions with the residues of Leu778, Leu1017, Ile1018, and Leu703. Usimine B docked best with the target protein (-7.3 kcal/mol) and established five H-bonds with Leu792, Met793, Asn842, Thr854, and Val843 residues as well as 10 hydrophobic interactions with the residues of Val726, Asn842, Thr855, Thr854, Leu844, Met793, Ala743, Leu718, Leu792 and Pro794 whereas the reference compound Gefitinib docked worst (-7.7 kcal/mol) and mediated seven H-bonds with the residues of Lys852, Gln791, Pro772, Asp1014, Asn771, Asp770 and Tyr1016 as well as five hydrophobic interactions with Gln791, Leu778, Arg776, Pro772 and Asn771 residues (Figure 2 (A)). Based on the binding energy and interacted amino acid residues as well as compared to the control (Gefitinib), Usimine B showed the best results in this experiment.

Table 3. Molecular docking analysis of Usimine A, Usimine B, and control compound (Gefitinib) with Brain Cancer (PDB ID: 5XDK).

Compound Name	Vina Score	Cavity Size	H-B interactions	Hydrophobic interactions
Control (Gefitinib)	-7.7	603	Lys852, Gln791, Pro772, Asp1014, Asn771, Asp770, Tyr1016	Gln791, Leu778, Arg776, Pro772, Asn771
Usimine A	-6.9	603	Ala1013	Leu778, Leu1017, Ile1018, Leu703
Usimine B	-7.3	603	Leu792, Met793, Asn842, Thr854, Val843	Val726, Asn842, Thr855, Thr854, Leu844, Met793, Ala743, Leu718, Leu792, Pro794

Usimine B has the greatest potential to create a protein complex based on the visualization of the EGFR protein's molecular docking data; this protein has a binding affinity value of -7.3 kcal/mol. Additionally, Usimine B has the most bonds. As such, it may serve as a criterion for the docking method's effectiveness [25], and Usimine B may be an effective EGFR protein inhibitor.

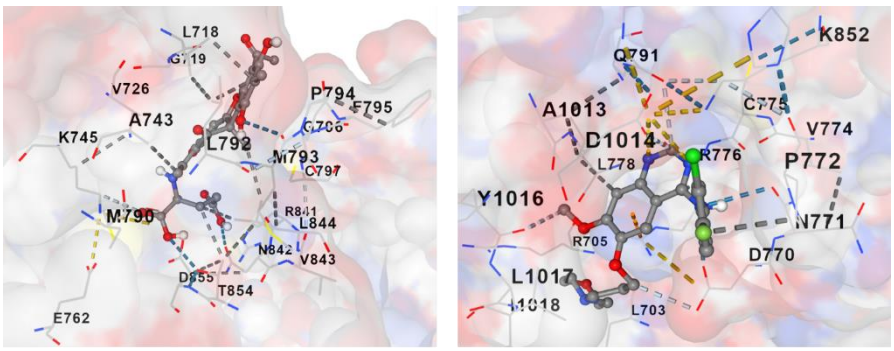

Figure 2. Molecular Docking interactions analysis of **(A)** lead compound (Usimine B); **(B)** control compound (Gefitinib).

3.4. Molecular Dynamic (MD) Simulation

Table 4. MD simulation of Cα atoms of apo EGFR, Usimine B-EGFR complex, and Gefitinib-EGFR complex.

System	RMSD (Å)	RMSF (Å)	RoG (Å)	SASA (Å^2)
Apo (Unbound)	2.84±0.27	13.72±4.44	20.43±0.11	15985.37±326.51
Min-Max	0-3.46	2.58-24.99	19.98-20.86	14633.69-17229.07
Usimine B-EGFR	2.26±0.23	12.21±3.69	20.36±0.11	15526.50±368.48
Min-Max	0-3.16	2.34-20.92	19.99-20.77	14189.98-16922.15
Gefitinib-EGFR	2.47±0.46	14.36±4.57	20.44±0.12	13980.90±465.98
Min-Max	0-3.76	2.70-21.89	20.03-20.95	13819.76-17112.76

For a chemical to have a long-lasting effect on its target, it must be stable in the binding pocket of the target [26]. Therefore, by calculating their RMSD during the course of the 200 ns simulation, we were able to examine the stability of Usimine B and Gefitinib inside the binding pockets of EGFR. The chemicals often cause primary and secondary structural disruptions when they attach to the targets, interfering with the targets' fundamental functions in the end [21]. Thus, we looked at the structural alterations that result from the active biomolecules binding to the proteins. On the Usimine B-EGFR and Gefitinib-EGFR complexes, the molecular dynamics simulation technique—which permits a time-scale examination of trajectories and coordinates—was applied. These were attained by obtaining the solvent accessible surface area (SASA) of Cα, radius of gyration (RoG), root mean square deviation (RMSD), and root mean square fluctuation (RMSF), which provide information about the compactness, flexibility, and stability of the simulated systems. The data of the MD simulation are presented in Table 4 and Figure 3.

The stability of the systems is reflected in the RMSD matric, which takes into account the variations of the Cα atoms in the residues. The stability of the Gefitinib-EGFR and Usimine B-EGFR complexes reached around 50 ns after the simulation began. With an average RMSD value of 2.84 ± 0.27 Å, the Apo protein demonstrated stability, but the Gefitinib-EGFR and Usimine B-EGFR complexes had average RMSD values of 2.47 ± 0.46 Å and 2.26 ± 0.23 Å, respectively (Figure 3 (A) and Table 4). Of all the complex systems, Usimine B showed the best stability when comparing the average RMSD values.

The EGFR protein's residual fluctuations are considered by the root-mean-square fluctuation (RMSF) of Cα. This matrix, which represents the protein's flexibility, may be used to estimate how much the protein is perturbed when chemicals bind to it. Because perturbations disrupt the normal functions of proteins, they can be used to infer the impact of biomolecules on their intended targets [21]. The protein's flexibility increases with greater RMSF values. Figure 3(B) illustrates that the apoprotein had an average RMSF value of 13.72 ± 4.44 Å,

whereas the Gefitinib-EGFR and Usimine B-EGFR complexes showed average values of 14.36 ± 4.57 Å and 12.21 ± 3.69 Å, respectively (Figure 3B and Table 4). These findings imply that by increasing the EGFR protein's flexibility, Usimine B and Gefitinib significantly disrupted the protein. Among the complex systems of EFGR, Usimine B demonstrated the least induced flexibility and the maximum stability according to the RMSD calculations.

We calculated the Radius of Gyration of the Cα atoms in the EGFR protein to further determine structural variations of the protein [27]. This matrix provides information on the proteins' compactness during the simulation period. High RoG values correspond to less compactness and vice versa [21]. Compared to the apoprotein and the Gefitinib-EGFR complex, the graph shown in Figure 3(C) indicated that the Usimine B-EGFR complex had the maximum compactness. Apo protein, the Usimine B-EGFR complex, and the Gefitinib-EGFR complex had average RoG values of 20.43 ± 0.11 Å, 20.36 ± 0.11 Å, and 20.44 ± 0.12 Å, respectively (Figure 3C and Table 4). The RMSF simulations, which show that less flexible systems are more compact than highly flexible systems, are consistent with these results.

The solvent-accessible surface area (SASA) is calculated using the interface that the solvent surrounds. Complexes interacting with the aqueous solution are more likely to occur in larger areas [28]. Furthermore, the variation of SASA reflects modifications in the buried area and the exposure of the protein surface. SASA fluctuations revealed that the Usimine B-EGFR complex had higher SASA values and displayed more volatility than the Gefitinib-EGFR combination.

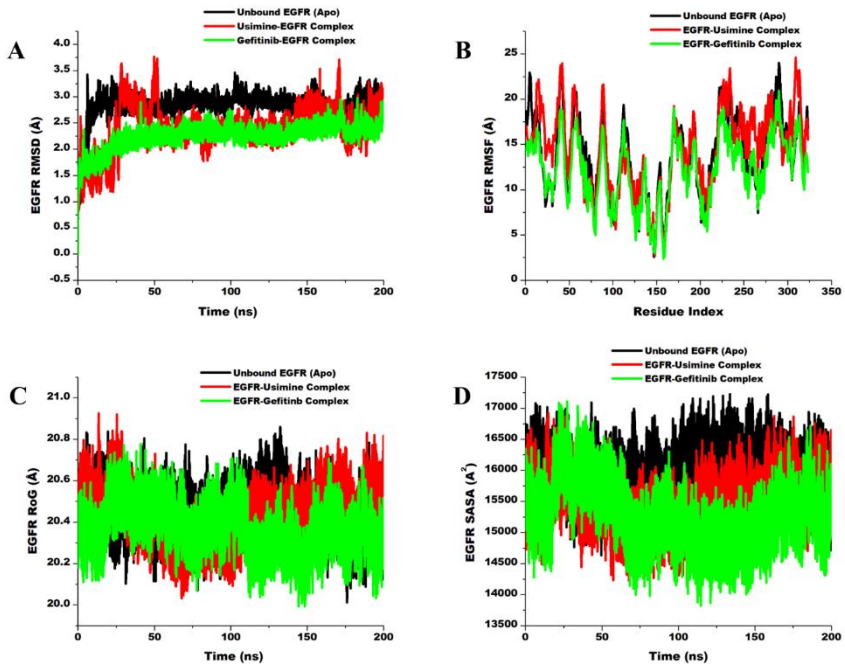

Figure 3. (**A**) Comparison of the RMSD plots of the Cα atoms in the apo EGFR, the usimine B-EGFR complex, and the Gefitinib-EGFR complex; (**B**) plots showing the individual residues of apo EGFR (black), the Usimine B-EGFR complex (red), and the Gefitinib-EGFR complex (green) comparing their RMSF values; (**C**) Gefitinib-EGFR complex (Green), Usimine B-EGFR complex (Red), and apo-EGFR's Cα atoms (Black) are shown in comparison using RoG; (**D**) Gefitinib-EGFR complex (Green), Usimine B-EGFR complex (Red), and apo-EGFR Cα atoms (Black) are plotted in a comparative SASA manner.

The results show that the SASA values of the apoprotein are 15985.37 ± 326.51 Å^2, whereas the complexes of Gefitinib-EGFR and Usimine B-EGFR have SASA values of 13980.90 ± 465.98 Å^2 and 15526.50 ± 368.48 Å^2, respectively (Figure 3(D) and Table 4). Based on the reported data, it is evident that Usimine B exhibited the highest level of stability

throughout the simulation period. This may account for its consistent ability to induce a stable, less flexible, and compact complex system compared to the other systems.

3.5. Trajectorial analysis of Usimine B-EGFR and Gefitinib-EGFR complexes during the simulation.

Molecular visualization of snapshots taken throughout the simulation was examined for the reference molecule, Gefitinib, and the lead compound, Usimine B. Based on this analysis, the residues that interacted with Usimine B and Gefitinib were Asp800, Met790, Gln791, Leu792, Gly796, Gly719, Met793, Arg841, Pro794, Leu718, Val726, Ala743, Cys797, Leu844 and Met793 (Figure 4). These interactions were caused by van der Waals, conventional hydrogen bonds, pi cation, and π-π, π-alkyl interactions. This kind of bond is observed to form between Usimine B's -OH and -CH_3 groups and the residues, particularly Met793, Arg841, and Leu844, highlighting their significance for the stability and interactions of the molecule. This may help explain its complicated high stability, low flexibility, and high compactness, as well as its comparatively high stability inside the binding pocket of EGFR protein.

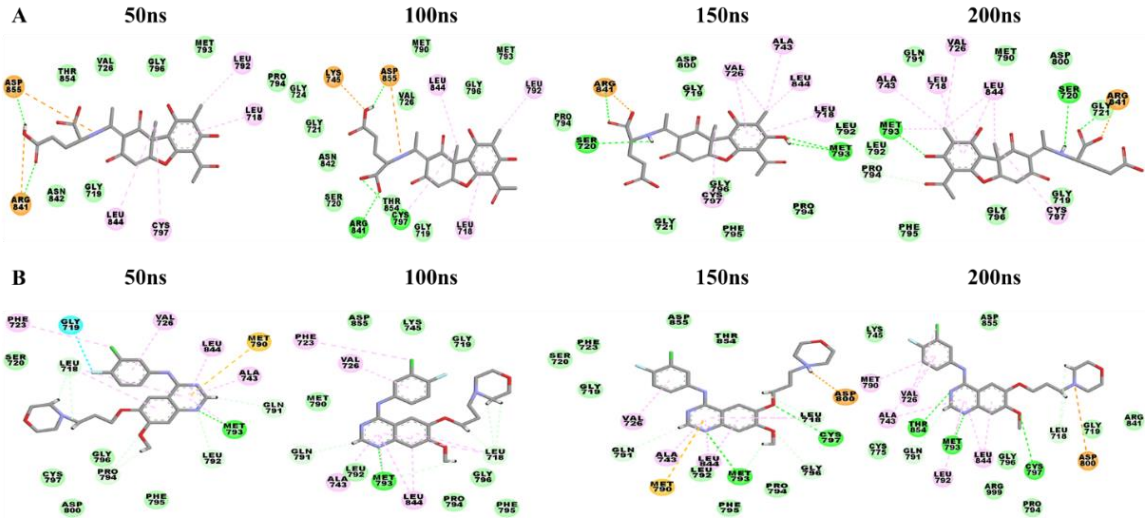

Figure 4. Interactions analysis of EGFR with **(A)** lead compound (Usimine B); **(B)** reference compound (Gefitinib) during 200 ns MD simulation.

3.6. Thermodynamics calculation.

Gefitinib-EGFR and Usimine B-EGFR complexes' free binding energy was examined using the MM/GBSA thermodynamics technique. This offers more details on the complexes' stability and binding energies. Free binding energies are a representation of the energy released during the creation of protein-ligand complexes. Greater binding energies suggest the production of undesirable complexes, whereas lower energies suggest the creation of favorable complexes. Based on the calculations shown in Table 5, the average binding energy ΔG for Gefitinib and Usimine B were found to be -31.09 ± 4.72 kcal/mol and -28.69 ± 3.50 kcal/mol, respectively. As a result, Usimine B had a binding energy that was similar to that of Gefitinib. These findings also support the same docking score of Usimine B and the stability that results within the binding pocket.

Table 5. The binding affinity of Usimine B-EGFR and Gefitinib-EGFR complexes using the MM/GBSA approach.

System	ΔE_{vdw}	ΔE_{ele}	ΔG_{gas}	ΔG_{sol}	ΔG_{bind}
Usimine B	-40.83 ±3.99	-59.65 ± 12.56	-100.48 ± 13.17	71.79 ± 11.66	-28.69± 3.50
Gefitinib	-38.66 ±3.87	-116.08 ± 24.98	-154.75 ± 24.67	123.65± 22.09	-31.09 ± 4.72

4. Conclusions

The findings of a computational study intended to find and create a novel inhibitor of brain cancer that targets the EGFR protein from Usimine A and Usimine B have been clarified by this research effort. PASS prediction, molecular docking, molecular dynamic modeling, and MM/GBSA inquiry investigations were also carried out to make them good and effective medicinal drugs. As agents for brain cancer, Usimine A had a 0.835<Pa<0.002 PASS prediction score, whereas Usimine B had a 0.851<Pa<0.002 score. These compounds' respective pIC50 values of 4.82 and 4.74 from the QSAR analysis suggested they would be therapeutically effective against the illness under investigation. Usimine B has strong binding affinities towards EGFR, as demonstrated by molecular docking studies, which provide docking scores of -7.3 kcal/mol. The 200 ns MD simulations demonstrated the stability of the Usimine B-EGFR complex compared to the reference complex. Furthermore, Usimine B showed a binding energy of -28.69 ± 3.50 kcal/mol in the active site of the EGFR protein of brain cancer. According to the present findings, Usimine B may be able to suppress the EGFR protein of brain cancer. Owing to the limitations of the experimental test, more in vivo and/or in vitro research on the compound Usimine B is strongly advised as a viable first step toward developing an EGFR inhibitor for brain cancer.

Funding

No.

Acknowledgments

The authors would like to thank the online software teams.

Conflicts of Interest

No.

References

1. Cheerlin Mishma, J.N.; Bena Jothy, V.; Narayana, B.; Kodlady, S.N.; Alharbi, N.S.; Abbas, G.; Muthu, S. Synthesis, DFT, solvent effect and biological attributes of NLO active 4-bromo-2-((2-(2,4-Dinitrophenyl) hydrazono)methyl) phenol -Potent drug anti-brain cancer. *J. Mol. Struct.* **2023**, *1289*, 135839, https://doi.org/10.1016/j.molstruc.2023.135839.
2. Zhou, D.; Gong, Z.; Wu, D.; Ma, C.; Hou, L.; Niu, X.; Xu, T. Harnessing immunotherapy for brain metastases: insights into tumor-brain microenvironment interactions and emerging treatment modalities. *J. Hematol. Oncol.* **2023**, *16*, 121, https://doi.org/10.1186/s13045-023-01518-1.
3. Speck-Planche, A.; V Kleandrova, V.; Luan, F.; Cordeiro, N.D.S. Chemoinformatics in Multi-target Drug Discovery for Anti-cancer Therapy: In Silico Design of Potent and Versatile Anti-brain Tumor Agents. *Anti-Cancer Agents Med. Chem.* **2012**, *12*, 678-685, http://dx.doi.org/10.2174/187152012800617722.
4. Guo, X.; Gao, C.; Yang, D.-H.; Li, S. Exosomal circular RNAs: A chief culprit in chemotherapy resistance. *Drug Resist. Updates* **2023**, *67*, 100937, https://doi.org/10.1016/j.drup.2023.100937.
5. Hyun, J. A Novel Association of *EGFR* Gene Alteration with Decreased Glioblastoma Patient Survival Rate. *Int. J. High School Res.* **2023**, *5*, 69-73.

6. Liu, M.; Yang, Y.; Wang, C.; Sun, L.; Mei, C.; Yao, W.; Liu, Y.; Shi, Y.; Qiu, S.; Fan, J.; Cai, X.; Zha, X. The effect of epidermal growth factor receptor variant III on glioma cell migration by stimulating ERK phosphorylation through the focal adhesion kinase signaling pathway. *Arch. Biochem. Biophys.* **2010**, *502*, 89-95, https://doi.org/10.1016/j.abb.2010.07.014.
7. Cornejo, A.; Salgado, F.; Caballero, J.; Vargas, R.; Simirgiotis, M.; Areche, C. Secondary Metabolites in *Ramalina terebrata* Detected by UHPLC/ESI/MS/MS and Identification of Parietin as Tau Protein Inhibitor. *Int. J. Mol. Sci.* **2016**, *17*, 1303, https://doi.org/10.3390/ijms17081303.
8. Paudel, B.; Bhattarai, H.D.; Lee, H.K.; Oh, H.; Shin, H.W.; Yim, J.H. Antibacterial activities of Ramalin, usnic acid and its three derivatives isolated from the Antarctic lichen *Ramalina terebrata*. *Z. Naturforsch. C. J. Biosci.* **2010,** *65*, 34-38, https://doi.org/10.1515/znc-2010-1-206.
9. Boustie, J.; Grube, M. Lichens—a promising source of bioactive secondary metabolites. *Plant Genet. Res.* **2005**, *3*, 273-287, https://doi.org/10.1079/PGR200572.
10. Lee, S.G.; Koh, H.Y.; Oh, H.; Han, S.J.; Kim, I.-C.; Lee, H.K.; Yim, J.H. Human dermal fibroblast proliferation activity of usimine-C from Antarctic lichen *Ramalina terebrata*. *Biotechnol. Lett.* **2010**, *32*, 471-475, https://doi.org/10.1007/s10529-009-0191-2.
11. Kwofie, S.K.; Broni, E.; Asiedu, S.O.; Kwarko, G.B.; Dankwa, B.; Enninful, K.S.; Tiburu, E.K.; Wilson, M.D. Cheminformatics-Based Identification of Potential Novel Anti-SARS-CoV-2 Natural Compounds of African Origin. *Molecules* **2020**, *26*, 406, https://doi.org/10.3390/molecules26020406.
12. Uddin, M.J.; Ali Reza, A.S.M.; Abdullah-Al-Mamun, M.; Kabir, M.S.H.; Nasrin, M.S.; Akhter, S.; Arman, M.S.I.; Rahman, M.A. Antinociceptive and Anxiolytic and Sedative Effects of Methanol Extract of *Anisomeles indica*: An Experimental Assessment in Mice and Computer Aided Models. *Front. Pharmacol.* **2018**, *9*, 246, https://doi.org/10.3389/fphar.2018.00246.
13. Nguyen, H.D.; Kim, M.-S. Identification of promising inhibitory heterocyclic compounds against acetylcholinesterase using QSAR, ADMET, biological activity, and molecular docking. *Comput. Biol. Chem.* **2023**, *104*, 107872, https://doi.org/10.1016/j.compbiolchem.2023.107872.
14. Das, N.R.; Sharma, T.; Goyal, N.; Singh, N.; Toropov, A.A.; Toropova, A.P.; Achary, P.G.R. Isoprenylcysteine carboxyl methyltransferase inhibitors: QSAR, docking and molecular dynamics studies. *J. Mol. Struct.* **2023**, *1291*, 135966, https://doi.org/10.1016/j.molstruc.2023.135966.
15. Zhu, Z.; Rahman, Z.; Aamir, M.; Shah, S.Z.A.; Hamid, S.; Bilawal, A.; Li, S.; Ishfaq, M. Insight into TLR4 receptor inhibitory activity *via* QSAR for the treatment of *Mycoplasma pneumonia* disease. *RSC Adv.* **2023**, *13*, 2057-2069, https://doi.org/10.1039/D2RA06178C.
16. Akash, S.; Mir, S.A.; Mahmood, S.; Hossain, S.; Islam, M.R.; Mukerjee, N.; Nayak, B.; Nafidi, H.-A.; Bin Jardan, Y.A.; Mekonnen, A.; Bourhia, M. Novel computational and drug design strategies for inhibition of monkeypox virus and *Babesia microti*: molecular docking, molecular dynamic simulation and drug design approach by natural compounds. *Front. Microbiol.* **2023**, *14*, 1206816, https://doi.org/10.3389/fmicb.2023.1206816.
17. Roney, M.; Singh, G.; Huq, A.K.M.M.; Forid, M.S.; Ishak, W.M.B.W.; Rullah, K.; Aluwi, M.F.F.M.; Tajuddin, S.N. Identification of Pyrazole Derivatives of Usnic Acid as Novel Inhibitor of SARS-CoV-2 Main Protease Through Virtual Screening Approaches. *Mol. Biotechnol.* **2024**, *66*, 696-706, https://doi.org/10.1007/s12033-023-00667-5.
18. Yan, X.E.; Zhu, S.J.; Liang, L.; Zhao, P.; Choi, H.G.; Yun, C.H. Structural basis of mutant-selectivity and drug-resistance related to CO-1686. *Oncotarget* **2017**, *8*, 53508-53517, https://doi.org/10.18632/oncotarget.18588.
19. Liu, Y.; Grimm, M.; Dai, W.-t.; Hou, M.-c.; Xiao, Z.-X.; Cao, Y. CB-Dock: a web server for cavity detection-guided protein–ligand blind docking. *Acta Pharmacol. Sin.* **2020**, *41*, 138-144, https://doi.org/10.1038/s41401-019-0228-6.
20. Roney, M.; Huq, A.K.M.M.; Issahaku, A.R.; Soliman, M.E.S.; Hossain, M.S.; Mustafa, A.H.; Islam, M.A.; Dubey, A.; Tufail, A.; Mohd Aluwi, M.F.F.; Tajuddin, S.N. Pharmacophore-based virtual screening and *in-silico* study of natural products as potential DENV-2 RdRp inhibitors. *J. Biomol. Struct. Dyn.* **2023**, *41*, 12186-12203, https://doi.org/10.1080/07391102.2023.2166123.
21. Rudrapal, M.; Issahaku, A.R.; Agoni, C.; Bendale, A.R.; Nagar, A.; Soliman, M.E.S.; Lokwani, D. *In silico* screening of phytopolyphenolics for the identification of bioactive compounds as novel protease inhibitors effective against SARS-CoV-2. *J. Biomol. Struct. Dyn.* **2022**, *40*, 10437-10453, https://doi.org/10.1080/07391102.2021.1944909.

22. Begam, B.F.; Kumar, J.S. Computer Assisted QSAR/QSPR Approaches – A Review. *Ind. J Sci. Technol.* **2016**, *9*, 1-8, https://dx.doi.org/10.17485/ijst/2016/v9i8/87901.
23. Muhammad, U.; Uzairu, A.; Ebuka Arthur, D. Review on: quantitative structure activity relationship (QSAR) modeling. *J. Anal. Pharm. Res.* **2018**, *7*, 240-242, https://doi.org/10.15406/japlr.2018.07.00232.
24. Kawsar, S.M.A.; Ferdous, J.; Hossain, M.K.; Kumer, A.; Akash, S.; Chakma, U. Molecular Docking against SARS-CoV-2 Variants, Antiviral, Dynamics and Quantum Chemical Modeling of Mannopyranoside Derivatives. *Mor. J. Chem.* **2023**, *11*, 897-1318, https://doi.org/10.48317/IMIST.PRSM/morjchem-v11i04.42045.
25. Nurhayati, A.P.D.; Rihandoko, A.; Fadlan, A.; Ghaissani, S.S.; Jadid, N.; Setiawan, E. Anti-cancer potency by induced apoptosis by molecular docking P53, caspase, cyclin D1, cytotoxicity analysis and phagocytosis activity of trisindoline 1,3 and 4. *Saudi Pharm. J.* **2022**, *30*, 1345-1359, https://doi.org/10.1016/j.jsps.2022.06.012.
26. Elhady, S.S.; Abdelhameed, R.F.A.; Malatani, R.T.; Alahdal, A.M.; Bogari, H.A.; Almalki, A.J.; Mohammad, K.A.; Ahmed, S.A.; Khedr, A.I.M.; Darwish, K.M. Molecular Docking and Dynamics Simulation Study of *Hyrtios erectus* Isolated Scalarane Sesterterpenes as Potential SARS-CoV-2 Dual Target Inhibitors. *Biology* **2021**, *10*, 389, https://doi.org/10.3390/biology10050389.
27. Shams Ul Hassan, S.; Abbas, S.Q.; Hassan, M.; Jin, H.Z. Computational Exploration of Anti-Cancer Potential of GUAIANE Dimers from *Xylopia vielana* by Targeting B-Raf Kinase Using Chemo-Informatics, Molecular Docking, and MD Simulation Studies. *Anti-Cancer Agents Med. Chem.* **2022**, *22*, 731-746, https://doi.org/10.2174/1871520621666211013115500.
28. Phanchai, W.; Srikulwong, U.; Chuaephon, A.; Koowattanasuchat, S.; Assawakhajornsak, J.; Thanan, R.; Sakonsinsiri, C.; Puangmali, T. Simulation Studies on Signature Interactions between Cancer DNA and Cysteamine-Decorated AuNPs for Universal Cancer Screening. *ACS Appl. Nano Mater.* **2022**, *5*, 9042-9052, https://doi.org/10.1021/acsanm.2c01337.